**The Thesis Committee for Vanessa J. Landsteiner**
**Certifies that this is the approved version of the following thesis:**

# Characterization of DAI during MCMV Infection

**APPROVED BY**
**SUPERVISING COMMITTEE:**

**Supervisor:**

Jason W. Upton

Haripriya Sridharan

# Characterization of DAI during MCMV Infection

**by**

**Vanessa J. Landsteiner, B.S.**

**Thesis**

Presented to the Faculty of the Graduate School of

The University of Texas at Austin

in Partial Fulfillment

of the Requirements

for the Degree of

**Master of Arts**

**The University of Texas at Austin**

**August 2015**

# Acknowledgements

I am eternally grateful to my advisor Dr. Jason Upton for his guidance and support throughout graduate school. His taught me to think in a different way and motivated me to become a better scientist.

I also want to thank Dr. Priya Sridharan, Katie Fennell and Adam Hilterbrand for being tremendous resources for problem solving experimental strategies and providing excellent technical training. Additional thanks to Sandhya Gopal, Jr. Perez and Katie Ragan for being supportive lab mates and creating a positive lab environment.

# Abstract

## Characterization of DAI during MCMV Infection

Vanessa J. Landsteiner, M.A.

The University of Texas at Austin, 2015

Supervisor: Jason W. Upton

Pathogen recognition initiates host cell defense mechanisms including activation of the innate immune system in an effort to clear an infection. As a survival mechanism, viruses have developed potent strategies to evade the host response. Viruses that persist for the life of their host, such as herpesviruses, are particularly adept at modulating host innate immunity to benefit the virus. Previous work has shown that receptor interacting protein kinase (RIP)3-dependent programmed necrosis is a critical host response toward murine cytomegalovirus (MCMV) infection, and this pathway is actively inhibited during infection by the MCMV M45 gene product, also known as vIRA. IRA inhibits the association of RIP3 with the DNA-dependent activator of interferon regulatory factors (DAI/ZBP-1), clearly implicating DAI in this pathway. In addition to programmed necrosis, DAI has also been implicated in the antiviral immune response toward herpesviruses. However, the mechanisms by which DAI mediates these functions during viral infection remain largely unexplored. Using the MCMV model, we have further characterized the role of DAI in the host innate immune response to MCMV infections.

Table of Contents

# List of Tables

# List of Figures

# Chapter 1: Introduction

Viruses are obligate intracellular parasites that can infect all organisms. They require access to host cell machinery in order to produce progeny virus. This necessity causes a battle between host and virus to evolutionarily outwit their opponent for better survival. Mammalian antiviral defense is a multifaceted immune response initiated through pattern recognition receptors (PRRs) of the innate immune system that recognize microbial pathogen-associated molecular patterns (PAMPs) (Broz and Monack, 2013). Binding of a PAMP by a PRR initiates signal cascades inducing downstream transcription factors, such as NF-κB and AP-1, that coordinate to upregulate expression of antiviral effectors, including type I interferon (IFN) and the pro-inflammatory cytokines, chemokines, and costimulatory molecules that activate the host innate and adaptive immune responses. Chemokines are secreted to warn neighboring cells to prepare for invasion and inflammatory cytokines recruit phagocytes to clear infection and activate the programmed cell death pathway to combat invaders.

In contrast to other free-living pathogenic microbes such as bacteria and fungi that produce unique products like lipopolysaccharide or flagellin, viruses produce few specific components that distinguish them from their hosts. For this reason, many host mechanisms for sensing viruses tend to focus on the detection of virus-associated nucleic acids that are found outside of the nucleus (Kumar et al., 2009; Paludan and Bowie, 2013; Wu and Chen, 2014). Nucleic acid-sensing receptors can be either membrane-bound or localized to the cytosol and each receptor possesses either an RNA or DNA recognition motif. Host cells present toll-like receptors (TLRs) on their cell surface and in endosomes to sample extracellular contents for pathogens. Cells also contain cytosolic receptors such as AIM2-like receptors (ALRs), NOD-like receptors (NLRs) and RIG-I-like

receptors (RLRs) that, upon sensing nucleic acids, evoke an innate immune response to limit viral and bacterial infections by initiating antiviral, pro-inflammatory, and programmed cell death pathway (Wang et al., 2014).

## 1.1 FORMS OF PROGRAMMED CELL DEATH

As a host defense mechanism, programmed cell death can be an effective strategy for limiting the success of intracellular pathogens. Cell death can be accomplished via several methods primarily apoptosis and programmed necrosis.

### 1.1.a Apoptosis

Apoptosis is the systematic dismantling of the cell without invoking an inflammatory response, and is defined by characteristic chromosomal fragmentation, nuclear condensation, and membrane blebbing (Hengartner, 2000). Apoptosis is dependent upon the sequential and coordinated activity of specific cysteine-proteases called caspases that are activated by intrinsic stimuli resulting in the loss of mitochondrial integrity or via extrinsic stimuli, such as PRR or ligation of death receptors, release of cytochrome c and formation of the apoptosome (Bratton and Salvesen, 2010). Phagocytes dispose of the dismantled components of the apoptotic bodies.

While apoptosis is an effective host defense to limit viral infection, most viruses have adapted to encode numerous cell death suppressors (Best, 2008; Lamkanfi and Dixit, 2010). Large DNA viruses like herpesvirues, poxviruses, and adenoviruses have numerous anti-apoptotic strategies. Molluscum contagiosum virus (MCV), Equine herpesvirus 1 (EHV-1), Cytomegalovirus (CMV) and Kaposi's sarcoma-associated herpesvirus (KSHV) each encode viral FLICE-like inhibitory proteins (vFLIP) proteins (MC159, E8, vICA and K13 respectively) that block the activation of caspase-8 delaying

apoptosis (Mocarski et al., 2012). Herpes simplex virus (HSV) expresses an immediate early protein, ICP0, that in addition to inhibiting interferon regulatory factors, also prevents the production of RNase L to stave off the degradation of viral RNAs as a mechanism to prevent activation of cytosolic nucleic acid sensors (Sobol and Mossman, 2006). MCMV uses two proteins, vMIA and vIBO (m38.5 and m41.1 respectively) to target BAX and BAK to directly block mitochondrial apoptosis, and encodes a third protein, vICA (M36), that inhibits caspase 8 (reviewed in Everett and McFadden, 1999; Kaiser et al., 2013; Tait and Green, 2012).

### 1.1b Caspase-8-independent Programmed Necrosis

In an effort to limit viruses which encode apoptotic cell death suppressors, host cells have evolved secondary death pathways that work independent of caspase-8 (Handke et al., 2012). Programmed Necrosis is characterized by cell swelling, organelle damage and plasma membrane rupture that spills cytoplasmic contents into the extracellular space resulting in extensive inflammation (Kaiser et al., 2013). When caspase 8 function is compromised, programmed necrosis is initiated, and requires the activity of Receptor-interacting protein kinase (RIP)3 (Cho et al., 2009; He et al., 2009; Upton et al., 2010; Zhang et al., 2009). Death receptor (DR)-induced programmed necrosis (also called necroptosis) results in the formation of the necrosome, a complex of RIP3 and a related kinase, RIP1 (Festjens et al., 0000; Meylan and Tschopp, 2005). RIP1-RIP3 interact via a specific protein-protein interaction motif, known as a RIP homotypic interaction motif (RHIM) (Sun et al., 2002) that is critical for programmed necrosis (Cho et al., 2009; Mocarski et al., 2012; Upton et al., 2010). Other RHIM-dependent, RIP3-containing complexes, including RIP3 with DAI (Kaiser et al., 2008) or

the TIR-domain containing adapter-inducing interferon beta (TRIF) (Meylan et al., 2004), also lead to necroptosis in response to pathogen infections (Sridharan and Upton, 2014)(Figure 1). These complexes sponsor the association of RIP3 with MLKL, a downstream effector, to mediate programmed necrosis.

### 1.2 Viral Defenses Block Programmed Necrosis

Like inhibitors of apoptosis, some viruses encode inhibitors of programmed necrosis. The MCMV M45 gene encodes the viral inhibitor of RIP activation (vIRA) which inhibits DR or TRIF-dependent apoptosis, necroptosis, and virus-induced programmed necrosis within 8-12 hours post-infection (Mack et al., 2008; Upton et al., 2008; Upton et al., 2010). vIRA contains a RHIM and binds RIP3 during infection to inhibit necrosis (Upton et al., 2010). Recombinant MCMV viruses encoding vIRA with a mutation in the RHIM are unable to suppress premature cell death in normal host cells and are entirely attenuated in normal and immunocompromised hosts. Moreover, in RIP3-deficient mice, mutant M45 MCMV virus replication is normalized to levels comparable to WT MCMV virus, demonstrating that the death pathway induced by mutant M45 encoding MCMV infection is RIP3-dependent (Upton et al., 2008; Upton et al., 2010). MCMV's vIRA protein has been shown to disrupt the RIP3-DAI interaction, inhibit NF-κB activation and RIP3 autophosphorylation when DAI is overexpressed (Kaiser et al., 2008; Rebsamen et al., 2009). In the absence of vIRA RHIM-mediated inhibition, RIP3 interacts with DAI during MCMV infection. DAI-deficient mice restore mutant vIRA MCMV virulence *in vivo* similar to RIP3-deficient mice (Upton et al., 2012). Although significant attention has been devoted to understanding the mechanisms of RIP3 activation and activity during necroptosis, there are many unanswered questions

regarding how RIP3-dependent virus-induced programmed necrosis is initiated and how DAI functions in that pathway.

### 1.3 STRUCTURE OF DAI

DAI (also known as ZBP1 or DLM-1) was first described as a gene upregulated in mouse tumor stromal cells (Fu et al., 1999) and later identified as a cytosolic DNA sensor of the immune system. It is believed to be involved in signaling to initiate IFN-β expression in the innate immune responses by activating the interferon-regulatory factor (IRF)-3 and NF-κB pathways (Takaoka et al., 2007). DAI is constitutively expressed in many cell types and tissues, including spleen, thymus, liver, lung and heart as well as in macrophages, and like many other pathogen sensors, it can be robustly induced by interferons (Fu et al., 1999).

DAI is comprised of two nucleic acid binding domains, two or possibly three, RHIM-like repeats (Figure 2), and a C-terminal domain believed to associate with the IRF3 transcription factor (Figure 3) (Takaoka et al., 2007). However, how these features influence DAI function is only beginning to be elucidated. DAI is unique in that it contains two Z-DNA binding domains, Zα and Zβ, on the N-terminus of the protein. These motifs bind Z-form DNA, and only two host other proteins are known to contain Z-DNA binding domains, the adenosine deaminase ADAR1 (Brown et al., 2000; Herbert et al., 1997) and PZK protein kinase containing Z-DNA binding domains (Rothenburg et al., 2005). Vaccinia virus encodes an innate immune modulator designated E3L, that contains a Z-binding domain, to overcome the host response (Herbert et al., 1997). However, the function of the Z-DNA binding domains is unclear. Crystal structures from human DAI revealed that the Zα domain strongly resembles other Z-DNA binding

domains with long continuous α-helixes (Schwartz et al., 2001), but the Zβ domain, while maintaining the conserved core residues (Y145, N141 and W161), has a unique structure that distinguishes it from other Z-DNA binding domains. The Zβ kinked helix blend presents a unique binding mode to interact with the DNA backbone of B-DNA and convert it to Z-form DNA (Ha et al., 2008). The two DNA binding motifs of DAI can independently bind Z-DNA, although substrate binding is greatly increased when they are linked in tandem (Deigendesch et al., 2006). Interestingly, naturally occurring isoforms of DAI lack the Zα domain, and have different subcellular localization (Pham et al., 2006). Moreover, mutation to core DNA-binding residues of the Zα domain change the subcellular localization from fine, diffused puncta throughout the cytoplasm to large accumulations of mutant DAI in proximity of stress granules as seen naturally with ΔZα isoforms (Deigendesch et al., 2006). Despite significant attention to the DNA binding function of Z-DNA binding motifs, there remains little insight into their natural function *in vivo*.

DAI has been suggested to recognize cytosolic DNA and facilitate activation of both TANK-binding kinase 1 (TBK1) and IRF3 to induce expression of IFN-β during herpes simplex virus infection in murine fibroblasts (Furr et al., 2011; Takaoka et al., 2007). DAI may require its Z-DNA binding domains to be fully activated *in vivo* and it is purported to dimerize to activate the immune system (Wang et al., 2008). Similar activation of interferon occurs during human CMV infection in human foreskin fibroblasts (DeFilippis et al., 2010a; DeFilippis et al., 2010b). Both the nucleic acid binding domains and C-terminal domain of DAI have been suggested to be necessary for downstream IRF3-mediated gene expression in response to cytosolic synthetic DNA and HSV-1 infection in murine L929 cells (Takaoka et al., 2007; Wang et al., 2008). However, truncation of the Zα domain of human DAI did not affect the expression of

IFNβ when stimulated with synthetic poly dA:dT in HEK293T cells (Lippmann et al., 2008), and DAI was entirely dispensable for innate responses in other human cell types, suggesting species or cell type dependent function for DAI. Moreover, DAI-deficient mice have normal innate and adaptive immune responses to B-form DNA and DNA vaccination, suggesting DAI is dispensable for the host immune response to cytosolic DNA (Ishii et al., 2008).

In contrast, as described above, DAI has also been shown to participate in RIP3 RHIM-dependent programmed necrosis pathway during MCMV infection (Upton et al., 2010, 2012). In addition to its unique nucleic acid binding motifs, DAI contains three RHIM-like repeats, RHIMs A, B, and C (Kaiser et al., 2008). RHIM A and RHIM B of DAI have been shown to bind other RHIM-containing protein, and RHIM A appears to be the dominant functional RHIM mediating the majority of binding to RIP1 and/or RIP3 to activate NF-κB (Kaiser et al., 2008; Rebsamen et al., 2009). RHIM C is less well conserved (Figure 2), and is considered a putative RHIM as it has not been shown to be functional (Kaiser et al., 2008). At present, only RHIM A of DAI has been implicated in MCMV-induced programmed necrosis (Upton et al., 2012).

### 1.4 Rationale for Study

Since DAI-RIP3 complex is targeted by vIRA to abrogate cell death, infections with WT MCMV and M45*mut*RHIM MCMV can be used as a natural system to further characterize the domains of DAI during MCMV infection. While it has been clearly established that DAI plays an important role in MCMV-induced programmed necrosis throught it's interaction with RIP3, a complete understanding the contribution of DAI's different domains during MCMV-induced necrosis is lacking. Moreover DAI has been

classified as a DNA sensor and implicated in activation of NF-κB and IFN production, however it's role in these host responses against MCMV infection is also unknown. This study aims to 1) undertake a thorough structure-function analysis of DAI in order to gain insights into the mechanism of its role in virus-induced programmed necrosis, and 2) define DAI's contribution to host innate immune signaling during MCMV infection.

# Chapter 2: Experimental Design and Methods

## 2.1 Expression Vector Construct Mutagenesis

Wild type murine DAI isoform 1 DNA was cloned into pCMV10-3XFLAG vector (Sigma-Aldrich) using the BglII/XbaI restriction sites to introduce a N-terminal epitope tag. Mutations to DAI were introduced using specific primers (Table 1) using overlap extension PCR. The N-terminal epitope-tagged DAI was then cloned into the pQCXIH vector (Clonetech) using the NotI/BamHI restriction sites. All construct mutations were verified through sequencing with specific primers (Table 2).

## 2.2 CRISPR Knockout SVEC cell lines

Endogenous DAI was targeted for knockout using the RNA-guided CRISPR/Cas9 system. Guide RNAs were designed using the Zhang Lab target finder database (crispr.mit.edu) and CRISPR construct design by DKFZ German Cancer Research Center (e-crisp.org) for target sites at the 29$^{th}$ or 69$^{th}$ amino acid located in exon 2 of DAI. These positions correspond to nucleotides 173216940-173216959 (29) and 173216853-173216835 (69) of the NCBI Mus mucsculus Annotation Release 105 (NC_000068.7). Two oligo 60-mers (Table 3) were annealed and extended with Fusion polymerase (Thermo Scientific) to generate a 100bp product. gRNACloning vector (Mali et al., 2013) (a gift from George Church (Addgene plasmid # 41824)) was linearized with AflII. The linearized vector and oligo fragment were cloned by Gibson assembly. The gRNA_Cloning Vector, hCas9 Vector (Mali et al., 2013) (a gift from George Church (Addgene plasmid # 41815)), and the puromycin resistance containing pQXCIP vector were co-transfected into SVEC4-10 cells. 24-hours post-transfection cells were selected for puromycin resistance using 2μg/ml puromycin. Following outgrowth, single cells

were subcloned by limiting dilution. Clonal populations were surveyed for absence of DAI expression via Western blot using the rabbit anti-ZBP clone 887 antibody (Karayel et al., 2009) (a gift from Tillman Burckstummer and Giulio Superti-Furga, CeMM). Sequence specific mutations were confirmed by sequencing of PCR amplified genomic DNA. Fragments were cloned into pCR-Blunt vector (Invitrogen), transformed into DH5α competent cells and selected for Kanamycin resistance. DNA was prepared and sequenced using the ZBP Surveyor primer set (Table 3).

### 2.3 STABLE-EXPRESSING DAI MUTANT CELL LINES

pQCXIH retroviral expression vectors containing FLAG-tagged WT or DAI-mutants (Figure 3) were transfected along with VSV-G, TAT and JK3 vectors into HEK293T cells using GenJet InVitro Transfection Reagent (Signagen) as described in manufacturer's protocol. Cell media was changed 18 hours post-transfection and supernatant media was collected at 24 and 48 hours post-transfection. Supernatants were stored at -80°C then thawed, passed through a 0.45 μm filter, and applied along with 8μg/ml polybrene to a monolayer of SVEC4-10 CRISPR KO cells. Transduction was repeated twice over 2-day period. Transduced cells were allowed to recover for 24 hours then selected with 400 μg/ml hygromycin for 3 days then reduced to 200 μg/ml for maintenance treatment. DAI expression was confirmed by immunoblotting for FLAG epitope.

### 2.4 CO-IMMUNOPRECIPITATION

Media was removed and monolayer cells were washed with PBS then lysed with NP-40 lysis buffer (150mM NaCl, 50mMTris pH8.0, 1% NP40, Complete protease

inhibitor). Cells were collected and further lysed by five passes through a 26G needle. Lysates were centrifuged for 20 minutes at 12,000 RPM at 4°C. Supernatant was transferred to new tube and the appropriate equilibrated magnetic agarose-congugated Anti-HA (Pierce) or Anti-FLAG® M2 (Sigma-Aldrich) beads were added. Samples were agitated, end-over-end, overnight at 4°C. The supernatant was removed post-incubation and beads were washed extensively with lysis buffer. Beads were boiled for 5 minutes at 95°C in 2xSDS Sample buffer. Protein lysates were then separated electrophoretically via SDS-PAGE gels and subjected to immunoblotting.

### 2.5 IMMUNOBLOTTING

Protein lysates were electrophoretically separated on 8% SDS-PAGE gels and transferred via semi-dry electrophoretic transfer cell onto nitrocellulose blotting membranes for immunoblot detection. Membranes were blocked with a 5% Non-fat milk-TBST solution for 1 hour, washed with TBST then treated with the indicated antibodies for 1hr to overnight. Primary antibodies were removed, membranes were washed 3 times with TBST solution and either subjected to ECL reagent for antibody detection or treated with a secondary antibody. Antibodies used in these studies were: Mouse anti-FLAG-M2 peroxidase conjugate (Sigma-Aldrich), rabbit anti-cMyc- peroxidase conjugate (Sigma-Aldrich), rabbit anti-DAI clone 887 (Karayel et. al, 2009 European Journal Immuno. 39(7) 1929-36.) (a gift from Tillman Burckstummer and Giulio Superti-Furga, CeMM), rabbit anti-mouse RIP3 (Imgenex), mouse anti-β-actin, cloneAC-74 (Sigma-Aldrich), peroxidase labeled anti-Mouse IgG (H+L) (Vector Laboratories, Inc.), and peroxidase labeled anti-Rabbit IgG (H+L) (Vector Laboratories, Inc.). ECL Prime Western blotting reagents (Amersham) were used for antibody detection on autoradiography film.

## 2.6 Cell Viability Assays

SVEC CRISPR Stable cell lines expressing mutant DAI proteins were seeded at a density of $5x10^3$ cells/well in 96-well plates and grown overnight. Cells were treated for death pathway responses with combinations of the following reagents: dimethyl sulfoxide (DMSO), 25 ng/ml mouse TNF-α (PeproTech), 50 μM/ml zVAD-fmk (Enzo Life Sciences), 5μg/μl cyclohexamide (Acros Organics) and/or 30 μM Necrostatin-1 (Calbiochem). Cell viability was also assessed under MCMV infection conditions as follows: either 50 μl medium for mock treated or infected with 50 μl WT K181 MCMV or M45*mut*RHIM MCMV inoculum containing 10 pfu/cell (MOI: 10) and incubated 18-hours under normal cell culture conditions. Cell viability was assessed using 50 μl CellTiter-Glo Luminescent Cell Viability Assay (Promega) as previously described (Upton et al., 2010; Upton et al., 2012). A Synergy microplate reader (Bio-Tek) was used to record the endpoint luminescence.

## 2.7 Sample Generation

SVEC CRISPR Stable cell lines expressing mutant DAI proteins were grown under normal cell culture conditions. Cells were seeded in a series of five sets of 6-well plates at a density of $3x10^5$ cells/well and grown overnight. Cells were either mock treated or infected with WT MCMV at MOI of 5 and harvested at indicated time points. Mock-infected cells were harvested at 0.16 hours post-treatment and MCMV-infected cells were harvested at 0.16 hours, 3 hours, 6 hours, and 9 hours post-infection. At harvest, cells were washed with PBS then preserved with 1ml RNA Later solution (Ambion) and stored at 4°C awaiting RNA isolation.

### 2.8 RNA ISOLATION

Plates were removed from 4°C, RNA Later solution was removed, and cell monolayer was washed twice with PBS. Cells were harvested and total RNA was isolated using the MirVana Total RNA Isolation kit (Ambion) according to manufacturer's protocol.

### 2.9 REVERSE-TRANSCRIPTASE PCR

1000 ng total RNA was DNase treated for 1 hour at 37°C then used to generate cDNA via the Superscript III First-Strand Synthesis System for RT-PCR (Invitrogen). The kit was used with the supplied oligo $dT_{20}$ primers according to manufacture's protocol.

### 2.10 QUANTITATIVE REVERSE-TRANSCRIPTION PCR

qPCR was conducted on StepOnePlus Real-Time PCR System (Applied Biosystems) using Universal SYBR Green Supermix (BIO-RAD Laboratories) with primer sets for the target genes IL-6 and IFN-β previously described in (Kaiser et al., 2008; O'Donnell et al., 2005). Primer sequences are found in Table 4. Cycling conditions were as follows: 50°C for 2 minutes and 95°C for 2 minutes then 40 cycles at 95°C for 15 seconds and 60°C for 1 minute. Melt curves were determined by 95°C for 15 seconds, 60°C for 1 minute then temperature increase at 3° increments to 95°C and 95°C hold for 15 seconds.

Target gene mRNA expression levels were normalized to the expression of GAPDH. The relative mRNA expression fold changes were calculated by the $\Delta\Delta C_t$

method. Data graphed compared to initial timepoint ($T_{0.16}$) for each mutant construct and also compared each mutant against the corresponding EV at each time point.

### 2.12 Statistical Analyses

Statistical significance was evaluated by using the student's T-test. P-value of $p<0.05$ was considered to be statistically significant.

# Chapter 3: Results

## 3.1 Construction of DAI mutants

In order to address the role of DAI in the host response to MCMV infection, a panel of truncation and point mutants of murine DAI was constructed (Figure 3). To investigate the role of the DNA-binding motifs, truncations removing the N-terminal Zα domain (amino acids 1-75- ΔZα) and both the Zα and Zβ domains (amino acids 1-150 - ΔZαβ) were constructed. Additionally, point mutations were made altering the conserved DNA binding residues of the Zα and Zβ motifs from asparagine to aspartate and tyrosine to alanine (N46D/Y50A – mZα; N122D/Y126A – mZβ), similar to previously constructed human DAI mutants that abrogate DAI binding to DNA (Deigendesch et al., 2006). The C-terminal region of DAI has been purported to mediate Interferonβ induction by recruiting TBK1/IRF (Takaoka et al., 2007). To examine the contribution from the C-terminal region, a truncation was made removing the last 100 amino acids from the C-terminus, similar to a previously constructed DAI mutant (Takaoka et al., 2007) (ΔC). Takaoka and colleagues found that DNA binding required a.a.155-233, which they termed "D3," which lies C-terminally adjacent to the Zβ DNA-binding domain and encompasses RHIM A (Kaiser et al., 2008; Takaoka et al., 2007). To further explore the activity of the "D3" region (Takaoka et al., 2007) both of the DNA binding domains and the C-terminal region of DAI were removed (ΔZαβ ΔC).

Current dogma suggests RHIM A is a major contributor of virus-induced cell death but does not dismiss a possible role for RHIM B. To monitor involvement of RHIM B in MCMV-induced programmed necrosis and confirm RHIM A activity, four alanine substitution mutations were made to the core residues of the RHIM (Figure 2) independently in either RHIM A (mRA) or RHIM B (mRB) and in tandem (mRAB). This mutageneisis strategy has been previously used to define the roles of RHIMs (Sun et al.,

2002; Upton et al., 2010; Upton et al., 2012). To further solidify RHIM A as a major contributor of cell death, a series of "RHIM swap" mutations were generated to test positional specificity of RHIM activity. RHIM A sequence was exchanged in place of RHIM B in WT DAI to create a mutant DAI with two identical RHIM A motifs lacking RHIM B (RA-RA). Additional mutation was introduced into the original RHIM A domain to render a mutant DAI with one functional RHIM A domain in the RHIM B position (mRA-RA). Similarly, RHIM B was exchanged for RHIM A generating a mutant lacking RHIM A but containing two RHIM B motifs (RB-RB), and four alanine substitution mutations were added to disable the primary RHIM B motif (RB-mRB), Lastly, a DAI mutant was designed to switch the RHIM A motif with the RHIM B motif to generate a mutant containing functioning RHIM A and RHIM B domains in their opposing location (RB-RA). Figure 3 shows a schematic representation of the described mutants of DAI. The expression of these mutants proteins were confirmed by western blot (Figure 4, left panel), and all were shown to express to comparable levels.

### 3.2 Characterization of mutant DAI-RIP3 Binding

As RIP3 binding is critical for DAI-mediated MCMV-induced programmed necrosis (Upton et al., 2012), we used the constructed DAI mutants (Figure 3) to determine the role of each domain in interaction with RIP3. As previously shown (Kaiser et al., 2008; Rebsamen et al., 2009), WT DAI robustly interacts with RIP3 in transient transfection assays, whereas mRA DAI fails to co-immunoprecipitate with RIP3 (Figure 4). Consistent with the importance of RHIM A to the interaction, mRAB failed to bind RIP3. DAI mRB and mRC co-immunoprecipitated RIP3 as efficiently as WT DAI, indicating that they are not significant contributors to the DAI-RIP3 interaction (Figure

4). Similarly, neither specific mutations in the N-terminal DNA binding domains, nor truncations of the N- and/or C-terminus of DAI prevented DAI from co-immunoprecipitating RIP3, indicating that the RHIM containing central portion of DAI is sufficient to bind RIP3. Due to a labeling error, human mZβ was used instead of murine mZβ DAI. As expected, human mZβ still efficiently coimmunoprecipitated with murine RIP3. Murine Zβ resembles the human form of DAI encoding the same core binding residues as human DAI, and in a similar location. However, the linker space between Zα and Zβ is 20 amino acids longer in human (Ha et al., 2008; Schwartz et al., 2001). Regardless, it is fully expected that murine mZβ binds RIP3, and this is currently being confirmed. The DAI RA-RA and mRA-RA mutants pulled down RIP3 as efficiently as WT DAI, while RB-RB and RB-mRB failed to efficiently interact with RIP3, further solidifying RHIM A as the sole critical interacting motif in the RIP3-DAI interaction. Interestingly, DAI RB-RA, where the positions of RHIM A and B are swapped within the DAI protein, remained capable of co-immunoprecipitating RIP3 (Figure 4). Together, these results indicate that RHIM A of DAI is necessary to mediate RIP3 binding.

### 3.3 Construction and characterization of stable cell lines expressing mutant DAI

To investigate the role of DAI in MCMV-induced programmed necrosis, we generated a cell line in which endogenous DAI was knocked out and reconstituted with the mutant DAIs described above (Figure 3). This strategy was employed to ensure endogenous WT DAI would not skew results and allow the investigation of each specific domain in isolation. Moreover, a comparable reconstitution strategy was previously used to demonstrate the role of DAI RHIM A in necrosis (Upton et al., 2012). The CRISPR/Cas9 system was employed to target sequence within the second exon of DAI to

yield a knockout cell line, and the knockouts were generated in SVEC4-10 murine endothelial cells. These cells were selected because they are sensitive to MCMV-induced programmed necrosis, and constitutively express RIP3 and DAI (Upton et al., 2010; Upton et al., 2012). Following selection and subcloning, DAI defective SVEC lines 29-11 and 69-3 were shown to be deficient in DAI expression by Western blot compared to either parental SVEC4-10 or 29-2 control cells (Figure 5). Sequencing confirmed the introduction of mutations, which result in the truncation and subsequent elimination of DAI expression (Figure 6). 29-11 and 69-3 were then used to generate a panel of cell lines stably-expressing the FLAG-tagged WT and mutant DAI alleles described in Figure 3. Western blotting confirmed expression of each DAI mutant, as well as expression of RIP3 (Figure 7).

### 3.4 Characterization of DAI in Virus-Induced Cell Death and TNF-induced necroptosis

Upon confirmation that stable cell lines expressed both RIP3 and the introduced DAI mutants, we next assessed the function of each DAI mutant during MCMV-induced programmed necrosis. SVEC-DAI Cell lines were infected with either WT or M45*mut*RHIM MCMV and survival was assessed, as previously described (Upton et al., 2010; Upton et al., 2012). As expected, empty vector control (EV) reconstituted SVEC cells, which lack DAI expression, were insensitive to MCMV-induced programmed necrosis, while WT DAI expressing cells were as sensitive to this death pathway as the control SVEC4-10 cell line 29-2, which express endogenous DAI (Figure 5). SVECs reconstitution with mRA remained insensitive to death (Figure 8), consistent with previous reports that DAI RHIM A is necessary for MCMV-induced programmed necrosis (Upton et al., 2012). Double mutant mRAB, lacking both RHIM A and RHIM

B, as well as RB-RB and RB-mRB, which lack RHIM A, all fail to sensitize SVECs to MCMV-induced programmed necrosis, similar to mRA (Figure 8), further confirming the critical role of RHIM A in necrosis. Surprisingly, SVECs reconstituted with RA-RA or mRA-RA, which both contain and intact RHIM A sequence and bind RIP3, were relatively insensitive to MCMV-induced programmed necrosis, suggesting that RHIM A alone is not sufficient to mediate this pathway. Conversely, but equally surprising, mRB reconstituted SVECs were hypersensitive to MCMV-induced programmed necrosis (Figure 8), which may indicate that RHIM B could function as a negative regulator of programmed necrosis. mZα, ΔZα, or ΔC DAI sensitized cells to MCMV-induced death at levels comparable to mRB, indicating that deletion or mutation of the Zα domain or deletion of the C-terminus of DAI is dispensable. Additionally, mZβ, mZαmZβ, and ΔZαmZβ DAI also sensitize cells to death during infection. These results suggest MCMV-induced programmed necrosis may not require DNA binding by DAI in murine endothelial cells. However, deletion of the Zβ domain in the context of ΔZαβ and ΔZαβΔC mutants, both of which retain the ability to bind RIP3 (Figure 4), partially or completely rescues from death, suggesting some feature of the Zβ region, independent of DNA– binding may be required to mediate virus-induced programmed necrosis. DAI-reconstituted cells were dying by RIP3-dependent, MCMV-induced programmed necrosis since treatment of infected cells with necrostatin 1 (Nec-1), a potent and selective inhibitor of RIP1 kinase activity (Degterev et al., 2005), did not influence virus induced death, as previously described (Upton, 2010#35). As controls, we also tested the panel of reconstituted cell lines for TNF induced necroptosis and apoptosis (Figure 9). DAI is not involved in TNF induced death, and consistently all of the above described cell lines, irrespective of their DAI status showed poor viability as compared to DMSO treated controls, when assayed for necroptosis (Figure 9A) or apoptosis (Fig 9B). Nec-1

rescued all of these cell lines from necroptotic death (Figure 9C). Interestingly, we noticed mRB and ΔC strongly sensitized cells to death when exposed to only zVAD or cycloheximide (Fig 9E,F), suggesting that RHIM B and the C-terminal region might negatively regulate DAI function. Similarly, all alleles lacking or mutated in the Zα region (mZα, ΔZα, mZα mZβ, and ΔZα mZβ) modestly sensitize cells to death in response to zVAD alone, again suggesting Zα may play a regulatory role in DAI function. Taken together, the results described above establish these cell lines as a valid tool to interrogate DAI's role in programmed necrosis and indicate that DAI RHIM A is necessary, but not sufficient, to mediate MCMV-induced programmed necrosis, that additional portions immediately adjacent to the Zβ domain are necessary, and that DAI DNA-binding may not be required.

### 3.5 Assessing DAI-dependent IFN and NF-κB activation during MCMV infection

To further explore the role of DAI in expression of IFN and NF-κB, we evaluated SVEC4-10 cells stably expressing DAI mutants to determine its contribution to these pathways. Initial experiments showed transfection of DAI-reconstituted SVEC4-10 cells with poly dA:dT showed an enhancement of IFNβ transcription compared to EV controls (Figure 10). This result is consistent with prior studies suggesting DAI mediates activation of IFN in response to cytosolic DNA (Takaoka et al., 2007). To extend these studies and assess the role of DAI in these pathways during MCMV infection, we infected the panel of WT and mutant DAI-reconstituted SVEC4-10 cell lines with WT MCMV at a high multiplicity, and determined mRNA levels of IFNβ and IL-6, an NF-κB responsive gene, by qPCR at various times post infection. Preliminary studies indicated that IFNβ and IL-6 levels peaked in infected parental SVEC4-10 cells within the first 9

hours post infection (data not shown). Surprisingly, there were no statistically significant differences found in IL-6 or IFNβ between EV and WT DAI-expressing SVECs during MCMV infection ($p > 0.05$) at the times assessed (Figure 11A, C). Similar results were obtained from all mutant DAI-reconstituted cell lines tested (Figure 11A-D). These results would suggests that DAI is not a significant contributor to the IFN or NF-κB pathways during MCMV infection.

# Chapter 4 Discussion

The work described here provides new insight into the mechanism of DAI function during MCMV infection. Previous work exploring the role of DAI in host responses used HSV-1, a human virus, in murine cell lines, as well as synthetic transfected DNA to elicit responses (Lippmann et al., 2008; Takaoka et al., 2007; Wang et al., 2008), leaving the interpretation of DAI function subject to artifacts of these unnatural systems. We developed a system of genetic knock-out and reconstitution of WT and mutant DAI expression in a biologically relevant context to systematically evaluate individual domains for their contribution to RIP3-mediated, virus-induced programmed necrosis. We further used this system to evaluate the potential role of DAI in pro-inflammatory and antiviral signaling during viral infection in a cell system originating from its natural host.

The data presented here corroborates previous findings (Kaiser et al., 2008; Rebsamen et al., 2009) that identified RHIM A of DAI as an important interacting motif necessary for RIP3 binding. RIP3 interaction with DAI can be maintained even when the position of RHIM A is shifted within the protein (Figure 4), although DAI encoding multiple copies of the RHIM A sequence show no evidence additional RIP3 binding. Truncating significant portions of the N- and C-termini of DAI does not diminish RIP3 interaction, and only mutation of RHIM A abrogates complex formation in transient assays. Together, these results clearly define RHIM A as necessary for DAI-RIP3 interaction. It is worth noting that the RB-RA mutant appears to show reduced binding to RIP3 (Figure 4), compared to RA-RA and mRA-RA mutants, suggesting that additional spatial considerations of the RHIMs within DAI warrant further investigation. One potential test of this hypothesis would be to generate additional DAI swap mutants,

including RHIM A replacing RHIM C location to ensure that the RIP3-DAI interaction is sequence specific regardless of the RHIM motif location.

One significant unexpected finding from this work was that although RHIM A of DAI is necessary for RIP3 interaction, it alone is not sufficient to mediate MCMV-induced programmed necrosis. The ΔZαβ and ΔZαβ ΔC truncation mutants contain an intact, correctly positioned RHIM A that is capable of interacting with RIP3 (Figure 4), however knock-out cells reconstituted with either were not sensitized to MCMV-induced necrosis (Figure 8). Similarly, the RHIM-swap mutations RA-RA and mRA-RA, while able to interact with RIP3, also failed to confer sensitivity to MCMV-induced necrosis (Figure 8). This is a surprising result in that RA-RA contains an intact, properly positioned RHIM A and binds RIP3 as efficiently as WT DAI, further supporting the idea that the spatial parameters of RHIMs within DAI influence their function. Together, these results demonstrate that RHIM A is critical for RIP3 binding, but additional structural or sequence features of DAI are necessary to mediate this death pathway.

To investigate the role of other domains in virus induced necrosis, we tested additional mutants designed to eliminate DAI binding to DNA (Figure 3) (Deigendesch et al., 2006). Interestingly, sensitivity to cell death was enhanced by mutants lacking the Zα DNA-binding domain (ΔZα) or when resides critical for DNA binding within the Z binding motifs were mutated (mZα, mZβ, and mZα mZβ) but not when both Zα and Zβ domains were removed (ΔZαβ) (Figure 9), implying that DNA binding to the Z-DNA binding motifs is not required for MCMV-induced cell death. Notably, the D3 region of DAI, as described by Takaoka and colleagues (Takaoka et al., 2007), is necessary for binding synthetic DNA *in vitro*. This region does not include the Z-DNA binding domains of DAI, but does encompass RHIM A, and is similar, but not identical, to the ΔZαβ DAI described here (Figure 3). ΔZαβ DAI removes a.a.1-175, whereas the DAI-

ΔN1 described by Takaoka and colleagues to define the D3 region, removes a.a.1-154 of DAI. To investigate this phenomenon further, DNA-binding assays are warranted to confirm whether ΔZαβ retains DNA binding capabilities and if DAI-ΔN1 is sufficient to sensitize cells to MCMV-induced programmed necrosis.

Another unanticipated result from this work is that mRB DAI enhances MCMV-induced programmed necrosis nearly 3-fold. The significant increase of cell death in cells containing mutant RHIM B but not when RHIM A is lacking (as in mRAB, RB-RB, and RB-mRB), suggests that RHIM B could possibly serve as a negative regulator of RHIM A. In our studies of the sensitivity of these cell lines to TNF-mediated necroptosis and apoptosis (Fig 9B), we found that mRB similarly increased sensitivity to zVAD or CHX alone. Curiously, in addition, we also observed that deletion of the regions of Zα and C-terminus also modestly sensitizes these cells to both treatments. Some accumulating evidence indicates that mutation of RHIM B enhances DAI-dependent activation of NF-κB (data not shown, (Rebsamen et al., 2009)), which in turn could enhance TNF production and secretion. However, it is also possible that mutations in the Zα, RHIM B, or C-terminus of DAI alter its structure or binding partner repertoire to affect some presently unappreciated facet of DAI signaling.

Due to conflicting reports as to the role of DAI in mediating type-I IFN and NF-κB responses to cytosolic DNA (Takaoka, 2007#133;Wang, 2008#130;Lippmann, 2008#129; Kaiser, 2008#37), we sought to clarify its role in these pathways during MCMV infection. Using our knock-out/reconstitution system, we found there were no significant differences between cells expressing no DAI and those expressing any mutant from our extensive panel. While we saw extensive variation in biological replicates that could be attributed to technical difficulties, our results indicate that DAI is not a major force in inducing NF-κB or IFN during MCMV infection of murine endothelial cells.

However, we have clearly shown it plays a significant role in mediating antiviral programmed necrosis. Although DAI may be involved in the host response during infection, it is not a dominant contributor to the induction of antiviral or pro-inflammatory cytokines during viral infection of a natural host. It is worth noting that most results indicating a role of DAI in these pathways were obtained in systems utilizing transfection of synthetic DNA or zoonotic infections (Lippmann et al., 2008; Takaoka et al., 2007; Wang et al., 2008). Our results support the notion that DAI may be a redundant or species-specific sensor of microbial infection.

## Figures and Tables

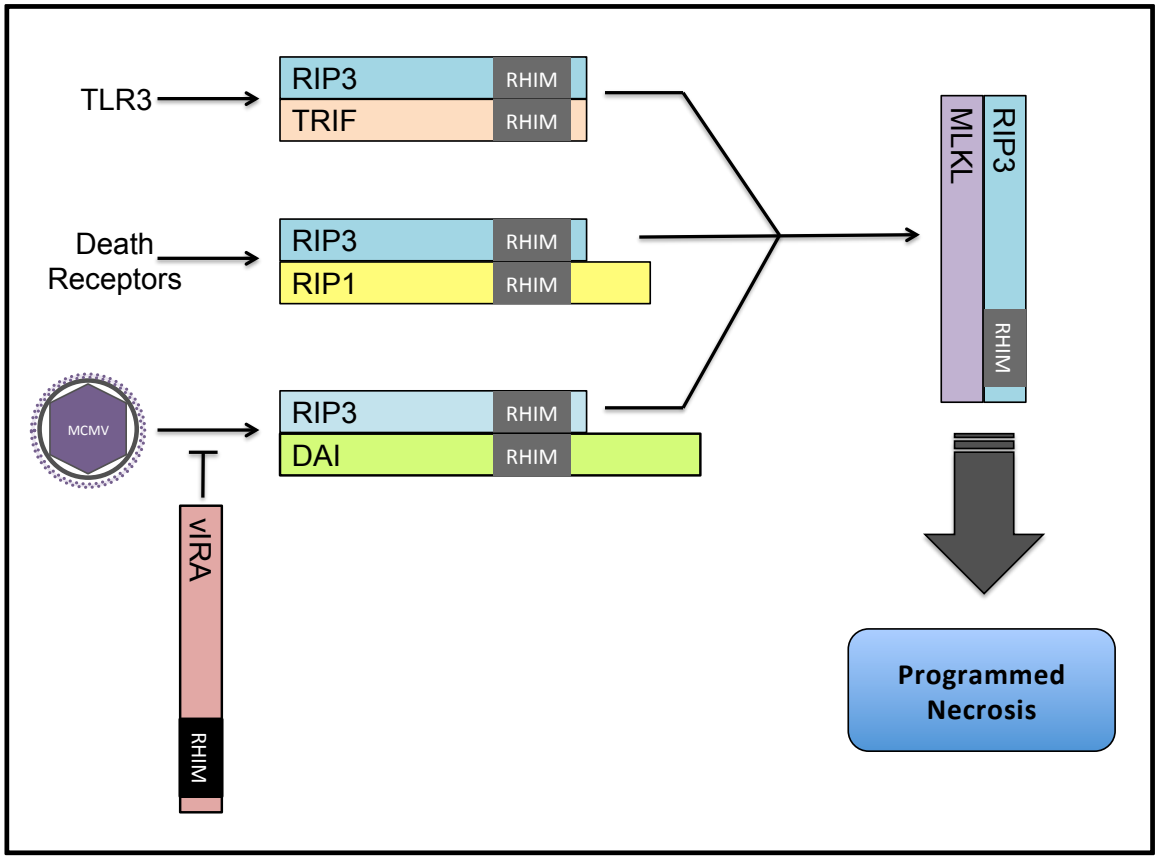


**Figure 1: Role of RHIM-containing proteins in programmed necrosis death signaling pathways.** TLR, death receptors, or viruses induce signaling by RHIM-containing adapters that activates programmed necrosis. RIP3 associates with either TRIF, RIP1 or DAI through homotypic interactions. MLKL is activated by the RHIM-RHIM protein complex and relays the signal downstream to initiate programmed necrosis. MCMV protein vIRA inhibits RIP3-DAI mediated signaling during infection by binding RIP3 to prevent complex formation. Abbreviations: RHIM, RIP homotypic interaction motif; TLR3, Toll-like receptor 3; RIP, receptor-interacting protein; TRIF, TIR domain-containing adapter-inducing interferon-β; MCMV, murine cytomegalovirus; MLKL, mixed lineage kinase domain-like; vIRA, viral inhibitor of RIP activation. Adapted from Sridharan & Upton, 2014.

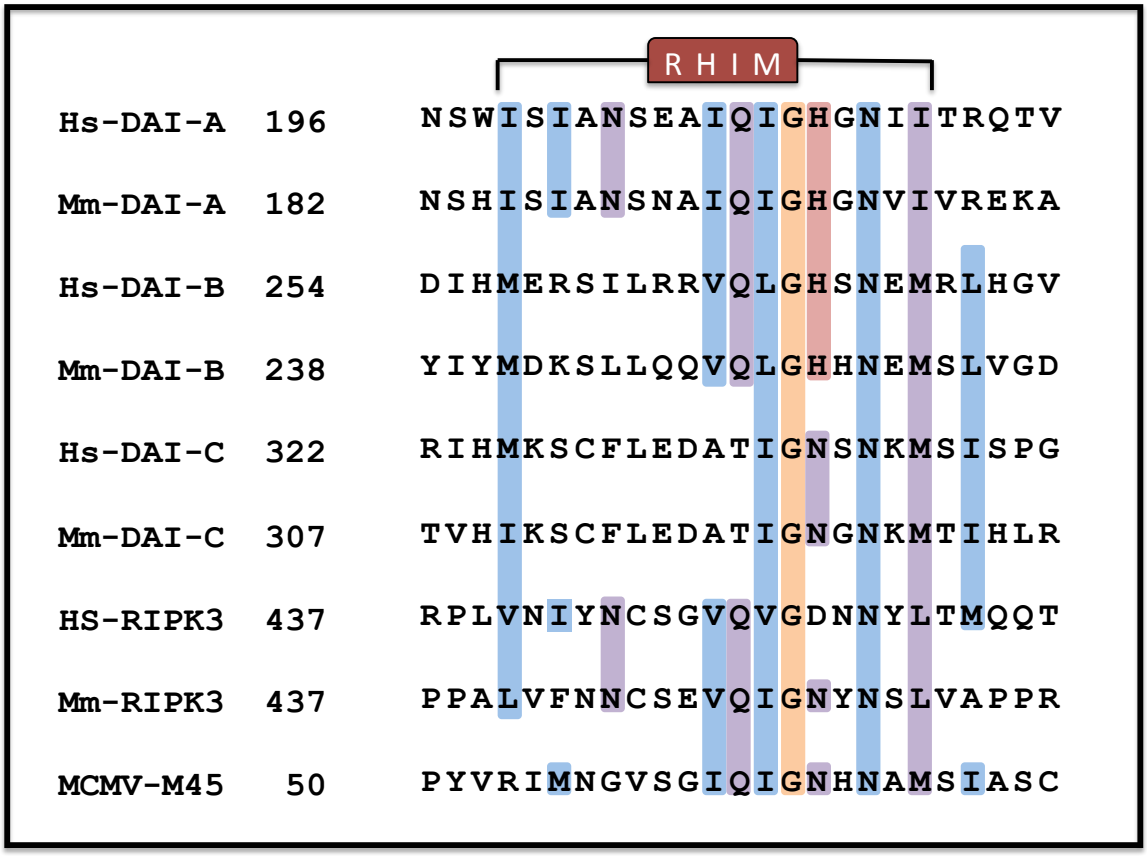


**Figure 2: Schematic representation of RHIM-containing proteins.** The RHIMs of human (Hs) and mouse (Mm) DAI and RIP3 kinase were aligned along with M45 gene of MCMV. Shaded regions represent a 60% identify threshold on the BLOSUM62 matrix. Adapted from Kaiser et. al, 2008.

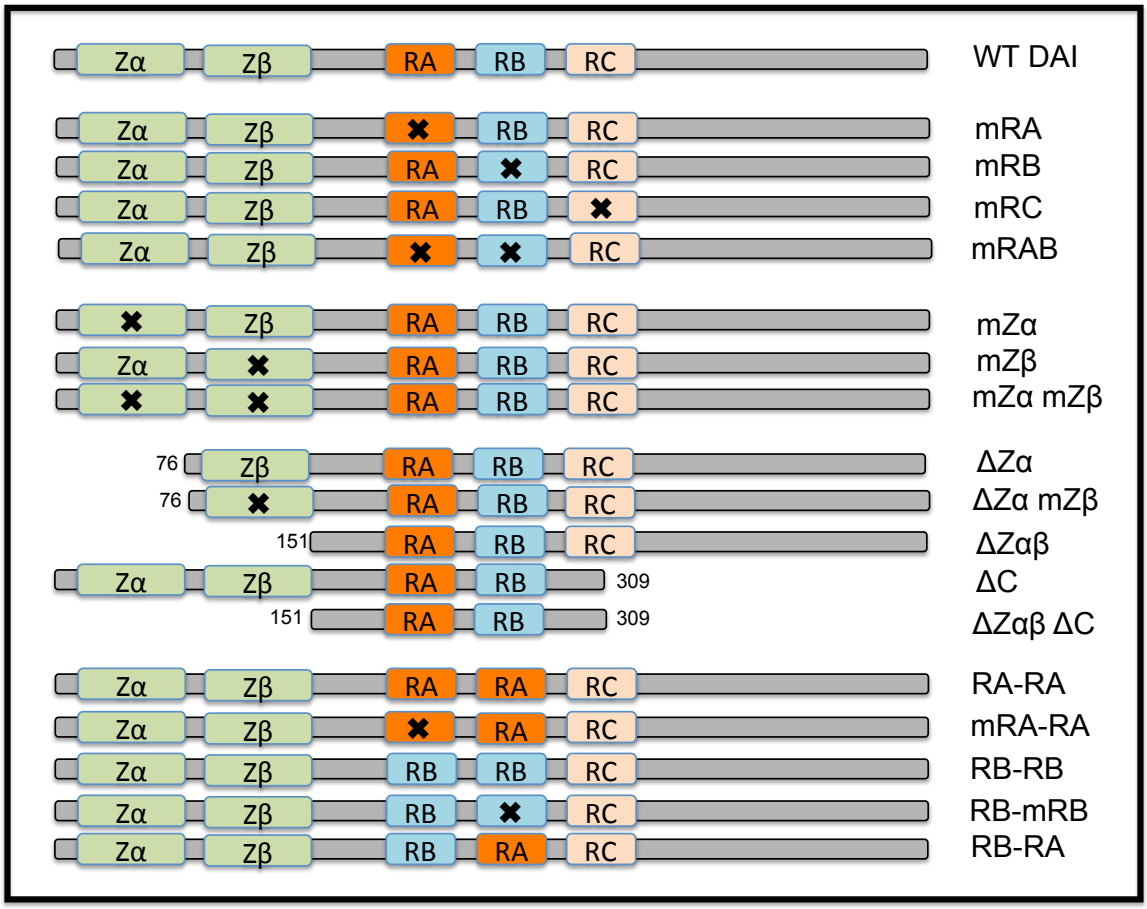


**Figure 3: Schematic representing DAI mutants used in these studies.** DAI contains two N-terminal Z-DNA binding domains (labeled Zα, Zβ) and three RHIM-like regions (labeled RA, RB, RC). Mutations are indicated with an ✖. Deletions are represented by missing icons. Amino acid positions are annotated next to deletions.

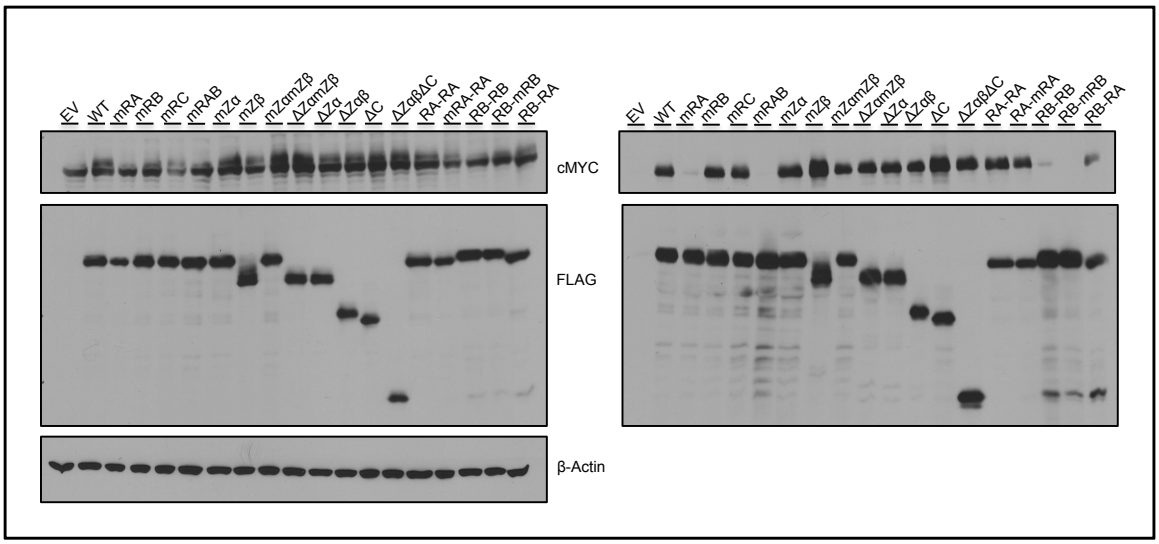


**Figure 4: DAI-RIP3 interaction requires RHIM A**. HEK293T cells transiently expressing 6MYC-RIP3 and the indicated 3Flag-DAI mutants. Cell lysates were subjected to immunoprecipitation (IP) with anti-Flag magnetic beads, and analyzed by immunoblot with anti-MYC, anti-FLAG, and anti-β-Actin. Whole cell lysate (WCL) left panel; FLAG IP right panel.

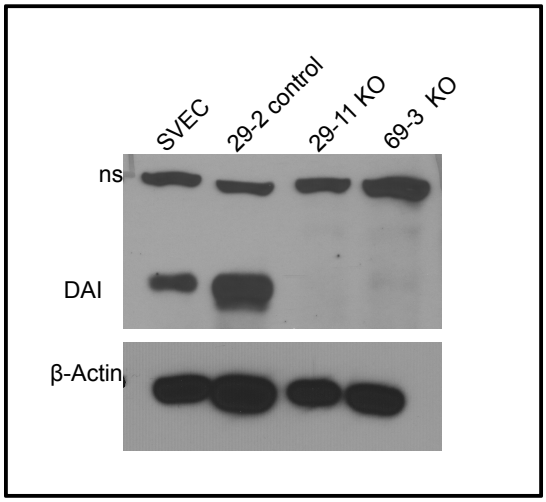


**Figure 5: Characterization of SVEC CRISPR Knockout cell lines deficient in DAI**. Cell lysates were prepared from the indicated parental, control, or knockout cell line, and analyzed by immunoblot to detect endogenous DAI and β-Actin.

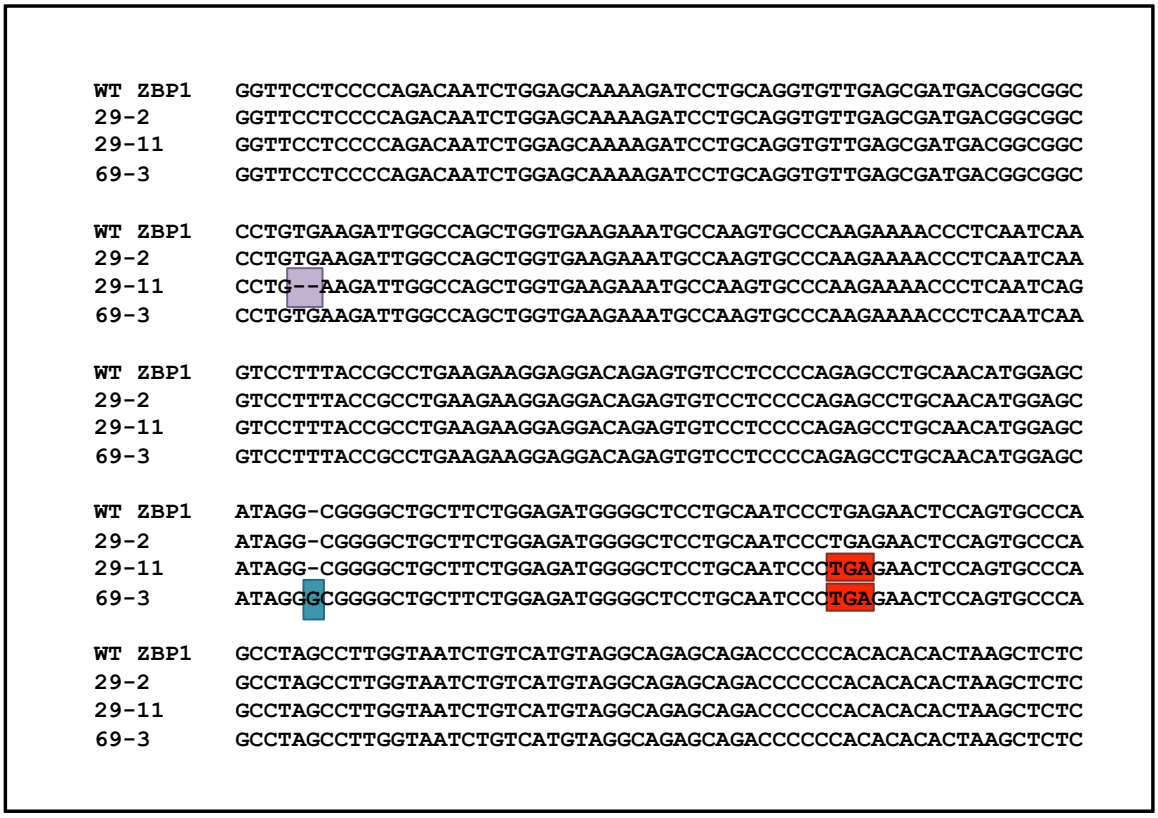


**Figure 6: Schematic representation of DAI mutations introduced through CRISPR/Cas9 system**. Nucleic acid sequences of 29-2 control, 29-11 KO or 69-3 KO cells aligned to murine DAI WT (gene ZBP1). Lavender shading highlights the two-base pair deletion in 29-11 and blue shading highlights the single base insertion in 69-3 cell line. Red shading highlights the resulting in-frame stop codon introduced by the mutations.

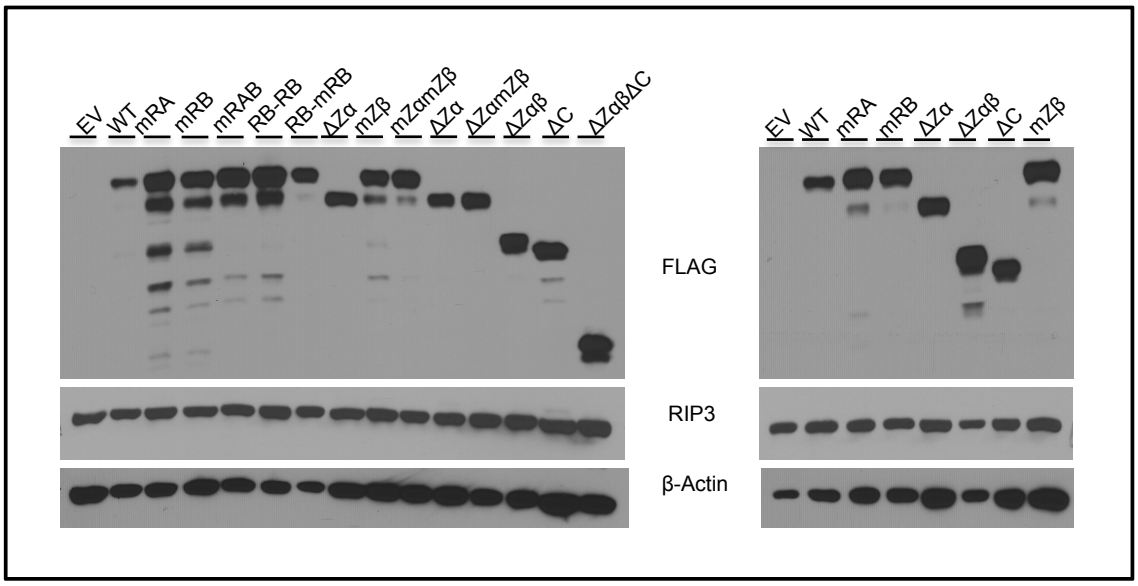


**Figure 7: Mutant DAI reconstituted in SVEC4-10 CRISPR KO.** Immunoblot analysis of WCL to detect Flag-tagged DAI mutants, endogenous RIP3, and β-actin from SVEC4-10 CRISPR KO cell lines reconstituted with Flag-DAI mutants. Clone 29-11 (left panel) and clone 69-3 (right panel).

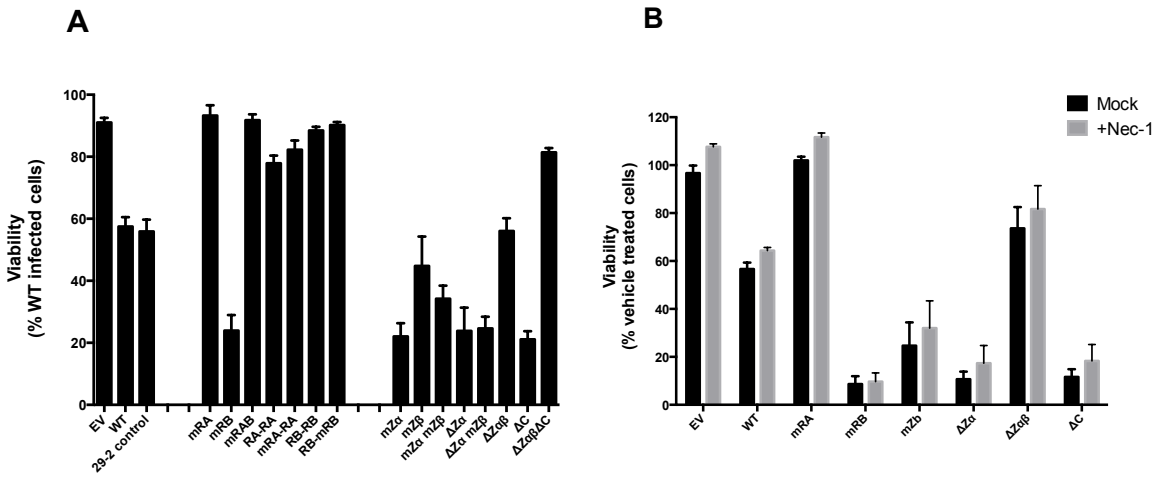


**Figure 8: Cell death responses of SVEC4-10 CRISPR KO cell lines**. A) Viability of indicated SVEC4-10 CRISPR KO reconstituted DAI mutant cell lines during MCMV infection (MOI=10). B) Viability of indicated SVEC4-10 CRISPR KO reconstituted DAI mutant cell lines with and without Nec-1 (30μM) treatment to inhibit RIP1 kinase activity. (n=3-6).

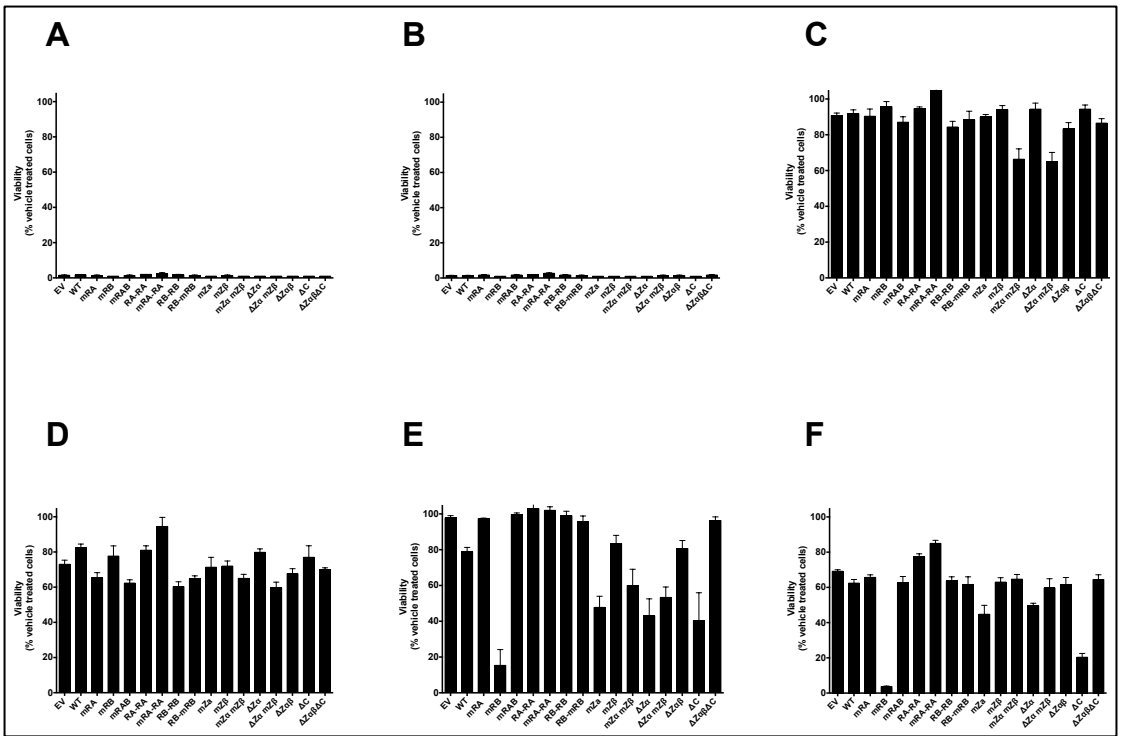


**Figure 9: SVEC4-10 stably expressing DAI Mutants remains sensitive to TNF-induced necroptosis and apoptosis**. Viability of mutant DAI-expressing SVEC4-10 stable cell lines after treatment with A) TNF (25ng/ml) and zVAD-fmk (50μM) to induce necroptosis. B) TNF (25ng/ml) and cyclohexamide (5μg/μl) to induce apoptosis C) TNF, zVAD-fmk and Nec-1 (30 μM) to inhibit RIP1-dependent cell death. Viability of mutant DAI-expressing SVEC4-10 stable cell lines after control treatments with D) TNF alone. E) zVAD-fmk alone. F) CHX alone. (n=3-12).

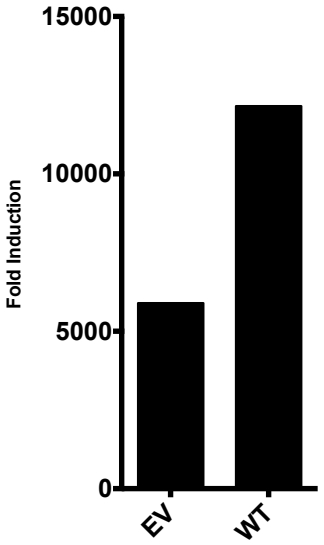


**Figure 10: Interferon-β induction after poly dA:dT stimulation.** SVEC4-10 knockout cells reconstituted with EV Flag control or WT DAI. Interferon-β induction measured by qPCR 9hrs post-treatment. (n=1).

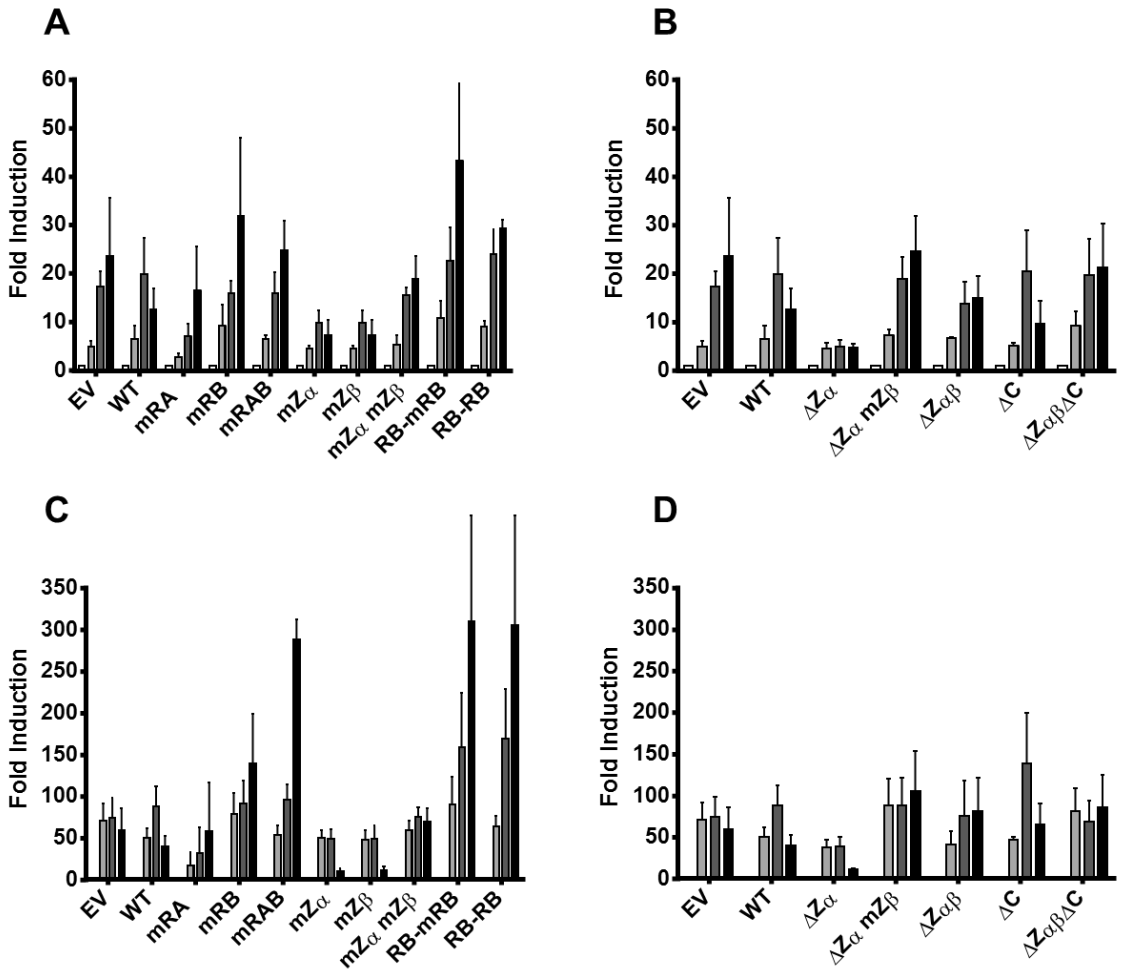


**Figure 11: NF-κB and Interferon-β induction during MCMV infection.** SVEC 29-11 knockout cells reconstituted with the indicated DAI mutants were infected with WT MCMV (MOI=5). Cells harvested at post-infection timepoints: 10 minutes ($T_{0.16}$ in white), 3 hours ($T_3$ in light grey), 6 hours ($T_6$ in dark grey), and 9 hours ($T_9$ in black) post-infection. Samples were normalized to $T_{0.16}$ and normalized timepoints are displayed for each DAI mutant indicated. EV and WT samples shown in B and D are the same data as in A and C respectively. (n=3-4). A) IL-6 induction in mutant DAI cells. B) IL-6 induction in DAI truncation cells. C) IFN-β induction in mutant DAI cells. D) IFN-β induction in DAI truncation cells.

Table 1. DAI Mutagenesis Primers

| Primer name | Sequence | Description |
|---|---|---|
| VL-005 | GAGAGGATCCAGCAGAAGCTCCTGTTGACTTGAGCA | Murine DAI orf to go into p3xFLAG-10 vector (Forward) |
| VL-006 | CGTAGGTACCTCATTGCTTGCTCAGTCCTGTGTC | Murine DAI orf to go into p3xFLAG-10 vector (Reverse) |
| VL-007 | TCCATTGCCAATTCAAACGCCGCCGCGGCTGCACACGGGAATGTCATAG | mRHIM A - Sense |
| VL-008 | CTATGACATTCCCGTGTGCAGCCGCGGCGGCGTTTGAATTGGCAATGGA | mRHIM A - Complement |
| VL-009 | TCCTTGCTCCAACAAGCGGCAGCTGCCCACCACAACGAGATGAGCCTC | mRHIM B - Sense |
| VL-010 | GAGGCTCATCTCGTTGTGGTGGGCAGCTGCCGCTTGTTGGAGCAAGGA | mRHIM B - Complement |
| VL-011 | CGTAGGTACCTCATAGAAAGCAGGATTTGATGTGGACTGTCTGG | dC - Complement |
| VL-016 | GAGAGGATCCAGGGGCTCCTGCAATCCCTGAGAAC | Zalpha truncation- Sense |
| VL-017 | GAGAGGATCCAGGCCAAGACATAGCTCATTCTGGA | Zalpha-beta truncation - Sense |
| VL-018 | TCCTGCTTTCTAGAGGACGCCGCCGCTGCAAACGGCAACAAGATGACC | mRHIM C - Sense |
| VL-019 | GGTCATCTTGTTGCCGTTAGCAGCGGCGGCGTCCTCTAGAAAGCAGGA | mRHIM C - Complement |
| VL-020 | GTGCCCAAGAAAACCCTCGATCAAGTGCTAGCCCGCCTGAAGAAGGAGG | mZalpha - Sense |
| VL-021 | CCTCCTTCTTCAGGCGGGCTAGCACTTGATCGAGGGTTTTCTTGGGCAC | mZalpha - Complement |
| VL-022 | AGCCAAAGAAGTCGACCCACTGCTAGCCTCCATGAGAAATAAGCA | mZbeta - Sense |
| VL-023 | TGCTTATTTCTCATGGAGGCTAGCAGTGGGTCGACTTCTTTGGCT | mZbeta - Complement |
| VL-024 | ATCTCTATAGCCAATTCAAACGCCATCCAGATTGGTCACGGGAATGTCAT AAGCCTCGTGGGGGATGCAG | RHIM A replaces RHIM B for RA-RA or mRA-RA constructs - Sense |
| VL-025 | TATGACATTCCCGTGACCAATCTGGATGGCGTTTGAATTGGCTATAGAGA TGTAGATGTACTGAGCTCCG | RHIM A replaces RHIM B for RA-RA or mRA-RA constructs - Complement |
| VL-026 | ATGGACAAGTCCTTGCTGCAGCAAGTGCAGCTTGGCCACCACAACGAGAT GGTAAGAGAGAAAGCCTGTGGTGAG | RHIM B replaces RHIM A for RB-RB or RB-mRB constructs -Sense |
| VL-027 | CATCTCGTTGTGGTGGCCAAGCTGCACTTGCTGCAGCAAGGACTTGTCCA TGTGGCTGTTGGCTCCTTGTTGG | RHIM B replaces RHIM A for RB-RB or RB-mRB constructs -Complement |

Table 2. DAI Sequencing Primers

| Primer name | Sequence | Description |
|---|---|---|
| VL-001 | AATGTCGTAATAACCCCGCCCCGTTGACGC | CMV30 primer for 3XFlag-CMV-10 plasmid -Sense |
| VL-002 | TATTAGGACAAGGCTGGTGGGCAC | CMV24 primer for 3XFlag-CMV-10 plasmid - Complement |
| VL-003 | ACGCCATCCACGCTGTTTTGACCT | pQCXIH - Sense |
| VL-004 | AAGCGGCTTCGGCCAGTAACGTTA | pQCXIH - Complement |

Table 3. CRISPR/Cas9 Primers

| Primer name | Sequence | Description |
|---|---|---|
| s-aa-69-S | TTTCTTGGCTTTATATATCTTGTGGAAAGGACGAAACACCGGCAACATGGAGCATAGGCG | CRISPR/Cas9 guide to 69th amino acid - Sense |
| s-aa-69-C | GACTAGCCTTATTTTAACTTGCTATTTCTAGCTCTAAAACCGCCTATGCTCCATGTTGCC | CRISPR/Cas9 guide to 69th amino acid - Complement |
| s-aa 29-S | TTTCTTGGCTTTATATATCTTGTGGAAAGGACGAAACACCGCCAGCTGGCCAATCTTCACA | CRISPR/Cas9 guide to 29th amino acid - Sense |
| s-aa 29-C | GACTAGCCTTATTTTAACTTGCTATTTCTAGCTCTAAAACTGTGAAGATTGGCCAGCTGGC | CRISPR/Cas9 guide to 29th amino acid - Complement |
| ZBP Surveyor FWD | CATAGTACACAGGGCAGGCTGTATAC | ZBP Surveyor sequencing - Sense |
| ZBP Surveyor REV | CTCAGATTTGAAGCCAAGCCTCGT | ZBP Surveyor sequencing - Complement |

Table 4. RT qPCR Primers

| Primer name | Sequence | Description |
|---|---|---|
| HS58 | TCCAGTTGCCTTCTTGGGAC | IL-6 Sense |
| HS59 | GTACTCCAGAAGACCAGAGG | IL-6 Complement |
| IFNb Fwd | GGAGATGACGGAGAAGATGC | IFN-b Sense |
| IFNb Rev | CCCAGTGCTGGAGAAATTGT | IFN-b Complement |
| GAPDH Fwd | TGTTCCTACCCCCAATGTGT | GAPDH Sense |
| GAPDH Rev | CCCAGTGCTGGAGAAATTGT | GAPDH Complement |

## References


Best, S.M. (2008). Viral Subversion of Apoptotic Enzymes: Escape from Death Row*. Annual Review of Microbiology *62*, 171-192.

Bratton, S.B., and Salvesen, G.S. (2010). Regulation of the Apaf-1–caspase-9 apoptosome. Journal of Cell Science *123*, 3209-3214.

Brown, B.A., Lowenhaupt, K., Wilbert, C.M., Hanlon, E.B., and Rich, A. (2000). The Z$\alpha$ domain of the editing enzyme dsRNA adenosine deaminase binds left-handed Z-RNA as well as Z-DNA. Proceedings of the National Academy of Sciences *97*, 13532-13536.

Broz, P., and Monack, D.M. (2013). Newly described pattern recognition receptors team up against intracellular pathogens. Nature reviews Immunology *13*, 551-565.

Cho, Y., Challa, S., Moquin, D., Genga, R., Ray, T.D., Guildford, M., and Chan, F.K.-M. (2009). Phosphorylation-Driven Assembly of the RIP1-RIP3 Complex Regulates Programmed Necrosis and Virus-Induced Inflammation. Cell *137*, 1112-1123.

DeFilippis, V.R., Alvarado, D., Sali, T., Rothenburg, S., and Fruh, K. (2010a). Human cytomegalovirus induces the interferon response via the DNA sensor ZBP1. Journal of virology *84*, 585-598.

DeFilippis, V.R., Sali, T., Alvarado, D., White, L., Bresnahan, W., and Fruh, K.J. (2010b). Activation of the interferon response by human cytomegalovirus occurs via cytoplasmic double-stranded DNA but not glycoprotein B. Journal of virology *84*, 8913-8925.

Degterev, A., Huang, Z., Boyce, M., Li, Y., Jagtap, P., Mizushima, N., Cuny, G.D., Mitchison, T.J., Moskowitz, M.A., and Yuan, J. (2005). Chemical inhibitor of nonapoptotic cell death with therapeutic potential for ischemic brain injury. Nat Chem Biol *1*, 112-119.

Deigendesch, N., Koch-Nolte, F., and Rothenburg, S. (2006). ZBP1 subcellular localization and association with stress granules is controlled by its Z-DNA binding domains. Nucleic acids research *34*, 5007-5020.

Everett, H., and McFadden, G. (1999). Apoptosis: an innate immune response to virus infection. Trends in Microbiology *7*, 160-165.

Festjens, N., Vanden Berghe, T., Cornelis, S., and Vandenabeele, P. (0000). RIP1, a kinase on the crossroads of a cell's decision to live or die. Cell Death Differ *14*, 400-410.

Fu, Y., Comella, N., Tognazzi, K., Brown, L.F., Dvorak, H.F., and Kocher, O. (1999). Cloning of DLM-1, a novel gene that is up-regulated in activated macrophages, using RNA differential display. Gene *240*, 157-163.

Furr, S.R., Chauhan, V.S., Moerdyk-Schauwecker, M.J., and Marriott, I. (2011). A role for DNA-dependent activator of interferon regulatory factor in the recognition of herpes simplex virus type 1 by glial cells. Journal of Neuroinflammation *8*, 99-99.

Ha, S.C., Kim, D., Hwang, H.Y., Rich, A., Kim, Y.G., and Kim, K.K. (2008). The crystal structure of the second Z-DNA binding domain of human DAI (ZBP1) in complex with Z-DNA reveals an unusual binding mode to Z-DNA. Proceedings of the National Academy of Sciences of the United States of America *105*, 20671-20676.

Handke, W., Krause, E., and Brune, W. (2012). Live or let die: manipulation of cellular suicide programs by murine cytomegalovirus. Med Microbiol Immunol *201*, 475-486.

He, S., Wang, L., Miao, L., Wang, T., Du, F., Zhao, L., and Wang, X. (2009). Receptor Interacting Protein Kinase-3 Determines Cellular Necrotic Response to TNF- $\alpha$ . Cell *137*, 1100-1111.

Hengartner, M.O. (2000). The biochemistry of apoptosis. Nature *407*, 770-776.

Herbert, A., Alfken, J., Kim, Y.-G., Mian, I.S., Nishikura, K., and Rich, A. (1997). A Z-DNA binding domain present in the human editing enzyme, double-stranded RNA adenosine deaminase. Proceedings of the National Academy of Sciences *94*, 8421-8426.

Ishii, K.J., Kawagoe, T., Koyama, S., Matsui, K., Kumar, H., Kawai, T., Uematsu, S., Takeuchi, O., Takeshita, F., Coban, C., *et al*. (2008). TANK-binding kinase-1 delineates innate and adaptive immune responses to DNA vaccines. Nature *451*, 725-729.

Kaiser, W.J., Upton, J.W., and Mocarski, E.S. (2008). Receptor-interacting protein homotypic interaction motif-dependent control of NF-kappa B activation via the DNA-dependent activator of IFN regulatory factors. Journal of immunology *181*, 6427-6434.

Kaiser, W.J., Upton, J.W., and Mocarski, E.S. (2013). Viral modulation of programmed necrosis. Current opinion in virology *3*, 10.1016/j.coviro.2013.1005.1019.

Karayel, E., Bürckstümmer, T., Bilban, M., Dürnberger, G., Weitzer, S., Martinez, J., and Superti-Furga, G. (2009). The TLR-independent DNA recognition pathway in murine macrophages: Ligand features and molecular signature. European Journal of Immunology *39*, 1929-1936.

Kumar, H., Kawai, T., and Akira, S. (2009). Toll-like receptors and innate immunity. Biochemical and biophysical research communications *388*, 621-625.

Lamkanfi, M., and Dixit, V.M. (2010). Manipulation of Host Cell Death Pathways during Microbial Infections. Cell host & microbe *8*, 44-54.

Lippmann, J., Rothenburg, S., Deigendesch, N., Eitel, J., Meixenberger, K., van Laak, V., Slevogt, H., N'Guessan P, D., Hippenstiel, S., Chakraborty, T., *et al*. (2008). IFNbeta responses induced by intracellular bacteria or cytosolic DNA in different human cells do not require ZBP1 (DLM-1/DAI). Cellular microbiology *10*, 2579-2588.

Mack, C., Sickmann, A., Lembo, D., and Brune, W. (2008). Inhibition of proinflammatory and innate immune signaling pathways by a cytomegalovirus RIP1-interacting protein. Proceedings of the National Academy of Sciences *105*, 3094-3099.

Mali, P., Yang, L., Esvelt, K.M., Aach, J., Guell, M., DiCarlo, J.E., Norville, J.E., and Church, G.M. (2013). RNA-Guided Human Genome Engineering via Cas9. Science *339*, 823-826.

Meylan, E., Burns, K., Hofmann, K., Blancheteau, V., Martinon, F., Kelliher, M., and Tschopp, J. (2004). RIP1 is an essential mediator of Toll-like receptor 3-induced NF-[kappa]B activation. Nature immunology *5*, 503-507.

Meylan, E., and Tschopp, J. (2005). The RIP kinases: crucial integrators of cellular stress. Trends in Biochemical Sciences *30*, 151-159.

Mocarski, E.S., Upton, J.W., and Kaiser, W.J. (2012). Viral infection and the evolution of caspase 8-regulated apoptotic and necrotic death pathways. Nature reviews Immunology *12*, 79-88.

O'Donnell, S.M., Hansberger, M.W., Connolly, J.L., Chappell, J.D., Watson, M.J., Pierce, J.M., Wetzel, J.D., Han, W., Barton, E.S., Forrest, J.C., *et al*. (2005). Organ-specific roles for transcription factor NF- $\kappa$ B in reovirus-induced apoptosis and disease. Journal of Clinical Investigation *115*, 2341-2350.

Paludan, S.R., and Bowie, A.G. (2013). Immune sensing of DNA. Immunity *38*, 870-880.

Pham, H.T., Park, M.Y., Kim, K.K., Kim, Y.G., and Ahn, J.H. (2006). Intracellular localization of human ZBP1: Differential regulation by the Z-DNA binding domain, Zalpha, in splice variants. Biochemical and biophysical research communications *348*, 145-152.

Rebsamen, M., Heinz, L.X., Meylan, E., Michallet, M.C., Schroder, K., Hofmann, K., Vazquez, J., Benedict, C.A., and Tschopp, J. (2009). DAI/ZBP1 recruits RIP1 and RIP3 through RIP homotypic interaction motifs to activate NF-kappaB. EMBO reports *10*, 916-922.

Rothenburg, S., Deigendesch, N., Dittmar, K., Koch-Nolte, F., Haag, F., Lowenhaupt, K., and Rich, A. (2005). A PKR-like eukaryotic initiation factor 2 $\alpha$ kinase from zebrafish contains Z-DNA binding domains instead of dsRNA binding domains. Proceedings of the National Academy of Sciences of the United States of America *102*, 1602-1607.

Schwartz, T., Behlke, J., Lowenhaupt, K., Heinemann, U., and Rich, A. (2001). Structure of the DLM-1-Z-DNA complex reveals a conserved family of Z-DNA-binding proteins. Nature structural biology *8*, 761-765.

Sobol, P.T., and Mossman, K.L. (2006). ICP0 Prevents RNase L-Independent rRNA Cleavage in Herpes Simplex Virus Type 1-Infected Cells. Journal of virology *80*, 218-225.

Sridharan, H., and Upton, J.W. (2014). Programmed necrosis in microbial pathogenesis. Trends in Microbiology *22*, 199-207.

Sun, X., Yin, J., Starovasnik, M.A., Fairbrother, W.J., and Dixit, V.M. (2002). Identification of a Novel Homotypic Interaction Motif Required for the Phosphorylation of Receptor-interacting Protein (RIP) by RIP3. Journal of Biological Chemistry *277*, 9505-9511.

Tait, S.W.G., and Green, D.R. (2012). Mitochondria and cell signalling. Journal of Cell Science *125*, 807-815.

Takaoka, A., Wang, Z., Choi, M.K., Yanai, H., Negishi, H., Ban, T., Lu, Y., Miyagishi, M., Kodama, T., Honda, K., *et al*. (2007). DAI (DLM-1/ZBP1) is a cytosolic DNA sensor and an activator of innate immune response. Nature *448*, 501-505.

Upton, J.W., Kaiser, W.J., and Mocarski, E.S. (2008). Cytomegalovirus M45 Cell Death Suppression Requires Receptor-interacting Protein (RIP) Homotypic Interaction Motif (RHIM)-dependent Interaction with RIP1. Journal of Biological Chemistry *283*, 16966-16970.

Upton, J.W., Kaiser, W.J., and Mocarski, E.S. (2010). Virus inhibition of RIP3-dependent necrosis. Cell host & microbe *7*, 302-313.

Upton, J.W., Kaiser, W.J., and Mocarski, E.S. (2012). DAI/ZBP1/DLM-1 complexes with RIP3 to mediate virus-induced programmed necrosis that is targeted by murine cytomegalovirus vIRA. Cell host & microbe *11*, 290-297.

Wang, X., Li, Y., Liu, S., Yu, X., Li, L., Shi, C., He, W., Li, J., Xu, L., Hu, Z., *et al*. (2014). Direct activation of RIP3/MLKL-dependent necrosis by herpes simplex virus 1 (HSV-1) protein ICP6 triggers host antiviral defense. Proceedings of the National Academy of Sciences of the United States of America *111*, 15438-15443.

Wang, Z., Choi, M.K., Ban, T., Yanai, H., Negishi, H., Lu, Y., Tamura, T., Takaoka, A., Nishikura, K., and Taniguchi, T. (2008). Regulation of innate immune responses by DAI (DLM-1/ZBP1) and other DNA-sensing molecules. Proceedings of the National Academy of Sciences of the United States of America *105*, 5477-5482.

Wu, J., and Chen, Z.J. (2014). Innate Immune Sensing and Signaling of Cytosolic Nucleic Acids. Annual Review of Immunology *32*, 461-488.

Zhang, D.-W., Shao, J., Lin, J., Zhang, N., Lu, B.-J., Lin, S.-C., Dong, M.-Q., and Han, J. (2009). RIP3, an Energy Metabolism Regulator That Switches TNF-Induced Cell Death from Apoptosis to Necrosis. Science *325*, 332-336.